International Journal of Electronic Engineering and Computer Science
Vol. 1, No. 1, 2016, pp. 14-27
http://www.aiscience.org/journal/ijeecs

Reduced Boundary Element Method for Liquid Sloshing Analysis of Cylindrical and Conical Tanks with Baffles

Kirill Degtyarev[1, *], Vasyl Gnitko[1], Vitaly Naumenko[2], Elena Strelnikova[1]

[1]Strength and Optimization Department, A. N. Podgorny Institute for Mechanical Engineering Problems of the Ukrainian Academy of Sciences, Kharkiv, Ukraine
[2]High Math Department, Ukrainian State University of Railway Transport, Kharkiv, Ukraine

Abstract

In this paper we consider vibrations of cylindrical and conical baffled fuel tanks partially filled with a liquid. The liquid is supposed to be an ideal and incompressible one and its flow introduced by the vibrations of a shell is irrotational. The problem of the fluid-structure interaction was solved using the single-domain and multi-domain reduced boundary element methods. The rigid baffled tanks with different annular orifices were considered. The dependencies of frequencies via the orifice radius at different values of filling level were obtained numerically for vibrations of the fluid-filled tanks with and without baffles.

Keywords

Fluid-Structure Interaction, Baffles, Liquid Sloshing, Free Vibrations, Boundary Element Method, Single and Multi-domain Approach, Singular Integral Equations

Received: May 23, 2016 / Accepted: June 7, 2016 / Published online: June 28, 2016

1. Introduction

Sloshing is defined as the motion of free surface of a liquid in a partially filled tank or container. The inadequate slosh suppression can lead to failure of spacecrafts. For example, the early Jupiter flight was unsuccessful because the stepped-pitch program has stepping intervals near the fundamental slosh frequency and the sloshing arisen thereinafter caused the vehicle to go out of control.

Since the launch of the early space rockets, controlling the slosh of liquid fuel within a launch vehicle has been a major design concern. Moreover, with today's large and complex spacecraft, a substantial mass of fuel is necessary to place them into orbit and to perform orbital maneuvers. Slosh control of propellant is so a significant challenge to spacecraft stability. Mission failure has been attributed to slosh-induced instabilities in several cases [1-2].

The most precise computation of the liquid motion and slosh forces involves solving complex equations of non-linear fluid mechanics and is extremely cumbersome.

When liquids slosh in a closed container one can observe the multiple configurations (modes) in which the surface may evolve. Commonly, the different modes can be defined by their wave number α (number of waves in circumferential direction) and by their mode number n.

In view of minimising the crucial loads, preventing structural failure and governing the fluid position within the tank, extensive experimental and theoretical studies have been carried out since several decades.

Baffles are commonly used as the effective means of suppressing the magnitudes of fluid slosh, apart from enhancing the integrity of the tank structure, although only a few studies have assessed roles of baffles design factor.

* Corresponding author
E-mail address: illuvatar_zmiiv@mail.ru (K. Degtyarev), basil@ipmach.kharkov.ua (V. Gnitko), elena15@gmx.com (E. Strelnikova), naumenko.vitaly@mail.ru (V. Naumenko)

The effect of size and location of baffle orifice on the slosh has been reported in only two studies involving rectangular [3] and a generic [4] cross-section tank. Popov et al in [3] studied the effect of size and location of the orifice of a transverse baffle using a 2-dimensional rectangular tank model. In this study the authors also investigated the effects of an equalizer and alternate baffle designs on the magnitude of transient slosh force and moments, and concluded that an equalizer has negligible effect on liquid slosh, while a multi orifice baffle behaves similar to a conventional single orifice baffle.

It would be noted that anti-slosh properties of baffles designs have been investigated through laboratory experiments employing small size tanks of different geometry [5-8]. These have generally studied damping properties from free oscillations or slosh under harmonic or single-cycle sinusoidal inputs.

The overview of the research on the topic [9-12] demonstrates that the dynamic response of structures containing the liquid can be significantly influenced by vibrations of their elastic walls and their interaction with the sloshing liquid. The most of research have described the fluid-structure interaction neglecting gravity effects. The considerable results were obtained in [9, 10]. Bermudez A. et al. considered in [9] vibrations of 2D elastic vessel partially filled by an incompressible fluid under the gravity force. Here the only 2D rectangular tank was under consideration. The research work [10] of Gavrilyuk I. et al. is devoted to the vibration analysis of baffled cylindrical shells, but both shells and baffles were rigid. In this work the authors used the analytical method. So there are some limitations in proposed methods, and each new form of tank will be required new investigations.

With respect to all the numerical work, which has been done, it is fair to say that there is still no fully efficient numerical method to deal with the sloshing in fluid-structure interactions of the baffled tanks.

The novelty of proposed approach consists in possibility to study the influence of both rigid and elastic baffles in the liquid-filled tanks in the form of shells of revolution of arbitrary meridian profiles and with different filling levels.

In practice, the effect of baffles usually can be seen after the baffle has been installed. The proposed method makes it possible to determine a suitable place with a proper height for installation of the baffles in tanks by using numerical simulation.

2. Problem Statement

Consider the shell structure with installed internal baffles for damping sloshing. The structure and its sketch are shown in Figure 1.

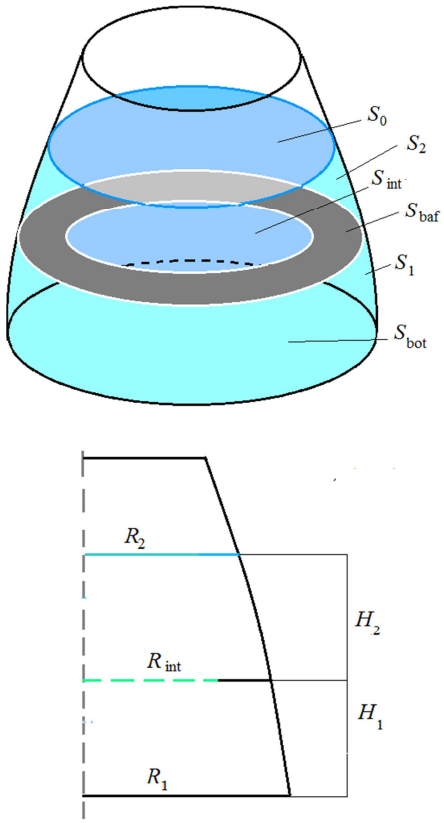

Figure 1. Shell structure with internal baffle.

Denote the wetted part of the shell surface through σ and the free surface of a liquid as S_0. The shell surface σ consists of four parts, $\sigma = S_1 \cup S_2 \cup S_{bot} \cup S_{baf}$. Here S_1 and S_2 are cylindrical surfaces of first and second fluid domains, S_{bot} is the surface of the tank bottom and S_{bot} is the baffle surface.

In this study the contained liquid is assumed to be inviscid and incompressible one and its flow induced by vibrations of the shell is irrotational.

Under these suppositions, there exists a velocity potential Φ defined as

$$V_x = \frac{\partial \Phi}{\partial x}; V_y = \frac{\partial \Phi}{\partial y}; V_z = \frac{\partial \Phi}{\partial z}.$$

This potential satisfies the Laplace equation.

The equations of motion of the two media (the shell, σ, and the fluid with the free surface, S_0, (see Fig.1)) can be written in the following form

$$\mathbf{L}(\mathbf{U}) + \mathbf{M}(\ddot{\mathbf{U}}) = \mathbf{P}, \quad (1)$$

where **U** is the vector-function of displacements, **P** is the fluid pressure on a moistened surface of the shell, and **L** and

M are the operators of elastic and mass forces.

Let us consider the right-hand side of Equation (1). Notice that the vector **P** points in the normal direction to the considered shell because an ideal fluid produces only a normal pressure on a moistened body. The modulus of vector **P** is denoted as $|\mathbf{P}| = p$. Assuming that the natural velocity of the fluid is zero, the value p, according to the Cauchy-Lagrange integral, can be represented as follows

$$p = -\rho_l \left(\Phi_t' + gz\right) + p_0 ,$$

where Φ is the velocity potential, g is the free fall gravity acceleration, z is the vertical coordinate of a point in the liquid, p_0 is the atmospheric pressure and ρ_l is the fluid density. To obtain the boundary equations on the free surface we have formulated dynamic and kinematics boundary conditions. The dynamic boundary condition consists in equality of the liquid pressure on the free surface to atmospheric one. The kinematics boundary condition requires that liquid particles of the free surface remain on it during all the time of subsequent motion. So

$$\left.\frac{\partial \Phi}{\partial n}\right|_{S_0} = \frac{\partial \zeta}{\partial t}; \quad p - p_0\big|_{S_0} = 0 ,$$

where an unknown function $\zeta = \zeta(t, x, y, z)$ describes the form and location of the free surface. Thus, we obtain the following boundary value problem to define the velocity potential Φ:

$$\nabla^2 \Phi = 0 , \left.\frac{\partial \Phi}{\partial \mathbf{n}}\right|_{\sigma} = \frac{\partial w}{\partial t} , \quad \left.\frac{\partial \Phi}{\partial \mathbf{n}}\right|_{S_0} = \frac{\partial \zeta}{\partial t}; \quad p - p_0\big|_{S_0} = 0 .$$

Here w indicates the normal component of the shell deflection, **n** is an external unit normal to the shell wetted surface namely, $w = (\mathbf{U}, \mathbf{n})$.

Reduce the problem under consideration to the following system of differential equations:

$$\mathbf{L}(\mathbf{U}) + \mathbf{M}(\ddot{\mathbf{U}}) = p\mathbf{n} ; \; p = -\rho_l \left(\frac{\partial \Phi}{\partial t} + gz\right) + p_0 ; \; \Delta\Phi = 0$$

with the next set of boundary conditions relative to Φ

$$\left.\frac{\partial \Phi}{\partial \mathbf{n}}\right|_{\sigma} = \frac{\partial w}{\partial t} , \left.\frac{\partial \Phi}{\partial \mathbf{n}}\right|_{S_0} = \frac{\partial \zeta}{\partial t} , \left.\frac{\partial \Phi}{\partial t} + gz\right|_{s_0} = 0$$

and fixation conditions of the shell relative to **U**.

To define coupled modes of harmonic vibrations let represent the vector **U** in the form $\mathbf{U}=\mathbf{u}\exp(i\omega t)$, where ω is an own frequency and **u** is a mode of vibration of the considered shell with a fluid.

3. The Mode Superposition Method for Coupled Dynamic Problems

Let seek modes of shell vibration with the liquid in the form

$$\mathbf{u} = \sum_{k=1}^{N} c_k \mathbf{u}_k , \tag{2}$$

where c_k are unknown coefficients and $\mathbf{u}_k$ are the normal modes of vibrations of the empty shell. In other words, a mode of vibration of the shell filled by fluid is determined as a linear combination of normal modes of its vibration without liquid.

The following relationships are fulfilled

$$\mathbf{L}(\mathbf{u}_k) = \Omega_k^2 \mathbf{M}(\mathbf{u}_k) , \quad (\mathbf{M}(\mathbf{u}_k), \mathbf{u}_j) = \delta_{kj} . \tag{3}$$

Hence

$$(\mathbf{L}(\mathbf{u}_k), \mathbf{u}_j) = \Omega_k^2 \delta_{kj} , \tag{4}$$

where Ω_k is the k-th frequency of empty shell vibrations. The above relationships show that the abovementioned shell's modes of vibration must be orthonormalized with respect to the mass matrix.

Represent Φ as a sum of two potentials $\Phi = \Phi_1 + \Phi_2$ as it was proposed by Gnitko V. et al. in [13]. Then represent the potential Φ_1 as the following series expansion

$$\Phi_1 = \sum_{k=1}^{N} \dot{c}_k \phi_{1k} . \tag{5}$$

Here time-dependant coefficients c_k are defined in Equation (2).

To determine φ_{1k} we have the following boundary value problems:

$$\Delta\phi_{1k} = 0 , \left.\frac{\partial \phi_{1k}}{\partial \mathbf{n}}\right|_{\sigma} = w_k , \; \phi_{1k}\big|_{S_0} = 0 . \tag{6}$$

Here $w_k = (\mathbf{u}_k, \mathbf{n})$. It would be noted that the solution of boundary value problem (6) was done in [14].

To determine the potential Φ_2 it is necessary to solve the problem of fluid vibrations in rigid vessel including gravitational force. It leads to following representation of potential Φ_2:

$$\Phi_2 = \sum_{k=1}^{M} \dot{d}_k \phi_{2k} \,, \tag{7}$$

where functions φ_{2k} are natural modes of liquid sloshing in the rigid tank. To obtain these modes we have solved the next sequence of boundary value problems:

$$\Delta\phi_{2k} = 0 \,;\; \left.\frac{\partial\phi_{2k}}{\partial\mathbf{n}}\right|_{S_1} = 0; \;\; \left.\frac{\partial\phi_{2k}}{\partial\mathbf{n}}\right|_{S_{\text{bot}}} = 0; \tag{8}$$

$$\left.\frac{\partial\phi_{2k}}{\partial n}\right|_{S_0} = \frac{\partial\varsigma}{\partial t}; \;\; \frac{\partial\phi_{2k}}{\partial t} + g\zeta = 0 \,. \tag{9}$$

Differentiated the second equation in relationship (9) with respect to t and substitute there the expression for ς_t' from the first one of (9). Suppose hereinafter that $\phi_{2k}(t,x,y,z) = e^{i\chi_k t}\phi_{2k}(x,y,z)$. Obtain the sequence of eigenvalue problems with following conditions on the free surface for each φ_{2k}:

$$\frac{\partial\phi_{2k}}{\partial n} = \frac{\chi_k^2}{g}\phi_{2k} \,. \tag{10}$$

The effective numerical procedure for solution of these eigenvalue problems using boundary element method was introduced in [13, 15].

Finally, the following relation for determining the potential Φ was obtained:

$$\Phi = \sum_{k=1}^{N} \dot{c}_k \phi_{1k} + \sum_{k=1}^{M} \dot{d}_k \phi_{2k} \,. \tag{11}$$

It follows from Equation (11) that function ζ can be written as

$$\zeta = \sum_{k=1}^{N} c_k \frac{\partial\phi_{1k}}{\partial n} + \sum_{k=1}^{M} d_k \frac{\partial\phi_{2k}}{\partial n} \,. \tag{12}$$

So, the total potential Φ satisfies the Laplace equation and non penetration boundary condition

$$\Delta\Phi = 0 \,;\; \left.\frac{\partial\Phi}{\partial\mathbf{n}}\right|_{\sigma} = \frac{\partial w}{\partial t}$$

due to validity of relations (6), (8). Noted that Φ also satisfies the condition

$$\left.\frac{\partial\Phi}{\partial\mathbf{n}}\right|_{S_0} = \frac{\partial\zeta}{\partial t}$$

as a result of representation (12).

When functions φ_{1k} and φ_{2k} are defined, substitute them in Equation (1) and obtain the system of the ordinary differential equations as it was done by E. Stelnikova et al. in [16].

4. Systems of the Boundary Integral Equations and Multi-domain Approach

To define functions φ_{1k} and φ_{2k} use the boundary element method in its direct formulation [17]. Dropping indexes $1k$ and $2k$ we can write the main relation in the form

$$2\pi\phi(P_0) = \iint_S q\frac{1}{|P-P_0|}dS - \iint_S \phi\frac{\partial}{\partial\mathbf{n}}\frac{1}{|P-P_0|}dS \,,$$

where $S = \sigma \cup S_0$.

In doing so, the function φ, defined on the surface σ, presents the pressure on the moistened shell surface and the function q, defined on the surface S_0, is the flux, $q = \dfrac{\partial\phi}{\partial\mathbf{n}}$.

To apply the multi-domain approach divide the fluid domain into two sub-domains Ω_1 and Ω_2 shown in Figure 2. Introduced the artificial interface surface S_{int}.

The boundaries of sub-domains Ω_1 and Ω_2 are denoted as $\Sigma_1 = S_{\text{bot}} \cup S_1 \cup S_{\text{baf}} \cup S_{\text{int}}$ and $\Sigma_2 = S_{\text{baf}} \cup S_{\text{int}} \cup S_1 \cup S_0$. The fluxes on interface surface will be denoted at both sides of the interface surface as $q_1 = \left.\dfrac{\partial\phi}{\partial\mathbf{n}}\right|_{S_{\text{int}}}$; $S_{\text{int}} \subset \Sigma_1$; $q_2 = \left.\dfrac{\partial\phi}{\partial\mathbf{n}}\right|_{S_{\text{int}}}$; $S_{\text{int}} \subset \Sigma_2$, and on the free surface we denote the flux as $q_0 = \left.\dfrac{\partial\phi}{\partial\mathbf{n}}\right|_{S_0}$.

Let introduce the next denominations: φ_1 and φ_2 are the potential values in nodes at the external boundaries of the tank in sub-domains Ω_1 and Ω_2 respectively.

The potential and flux values on the interface surface will be φ_{1i} and q_1, if $S_{\text{int}} \subset \Sigma_1$; and φ_{2i} and q_2 if $S_{\text{int}} \subset \Sigma_2$, respectively.

On the free surface denote the potential values in nodes as φ_0 and the flux values as $q_0 = \left.\dfrac{\partial\phi}{\partial\mathbf{n}}\right|_{S_0}$. The fluxes on the rigid surfaces are equal to zero.

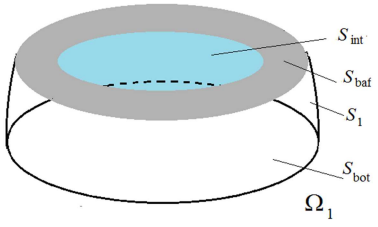

a)

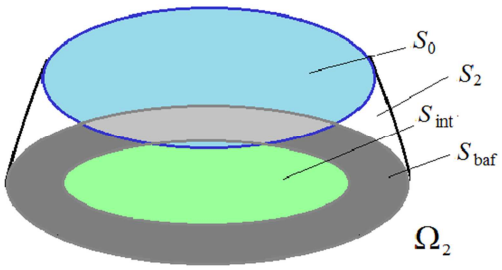

b)

Figure 2. Fluid sub-domains.

Introduce here the next denominations for rigid parts of the structure: $\sigma_1 = S_1 \cup S_{bot} \cup S_{baf}$ and $\sigma_2 = S_2 \cup S_{baf}$. On the interface surface S_{int} the next equalities are valid [17]:

$$\phi_{2i} = \phi_{1i}; \quad q_1 = -q_2 .$$

On the rigid parts the following conditions are valid $\left.\frac{\partial\phi}{\partial\mathbf{n}}\right|_{\sigma_1} = 0; \quad \left.\frac{\partial\phi}{\partial\mathbf{n}}\right|_{\sigma_2} = 0.$

Consider now the boundary value problem for determining the potential Φ_2. As in [13] using the relation $q_0 = \frac{\chi^2}{g}\phi_0$ and introducing the reduced frequency $\omega^2 = \frac{\chi^2}{g}$ we obtain the following system of singular integral equations:

$$\begin{aligned} &2\pi\phi_1(P_0) + \iint_{\sigma_1}\phi_1\frac{\partial}{\partial\mathbf{n}}\frac{1}{|P-P_0|}d\sigma_1 + \iint_{S_{int}}\phi_{1i}\frac{\partial}{\partial\mathbf{n}}\frac{1}{|P-P_0|}dS_{int} \\ &-\iint_{S_{int}} q_1\frac{1}{|P-P_0|}dS_{int} = 0; \quad P_0 \in \sigma_1; \end{aligned} \tag{13}$$

$$\begin{aligned} &2\pi\phi_{1i}(P_0) + \iint_{\sigma_1}\phi_1\frac{\partial}{\partial\mathbf{n}}\frac{1}{|P-P_0|}d\sigma_1 \\ &-\iint_{S_{int}} q_1\frac{1}{|P-P_0|}dS_{int} = 0; \quad P_0 \in S_{int} \end{aligned};$$

$$\begin{aligned} &2\pi\phi_2(P_0) + \iint_{\sigma_2}\phi_2\frac{\partial}{\partial\mathbf{n}}\frac{1}{|P-P_0|}d\sigma_2 + \iint_{S_{int}}\phi_{1i}\frac{\partial}{\partial\mathbf{n}}\frac{1}{|P-P_0|}dS_{int} \\ &+\iint_{S_{int}} q_1\frac{1}{|P-P_0|}dS_{int} + \iint_{S_0}\phi_0\frac{\partial}{\partial\mathbf{n}}\frac{1}{|P-P_0|}dS_0 \\ &-\omega^2\iint_{S_0}\phi_0\frac{1}{|P-P_0|}dS_0 = 0; \quad P_0 \in \sigma_2; \end{aligned}$$

$$\begin{aligned} &2\pi\phi_{1i}(P_0) + \iint_{\sigma_2}\phi_2\frac{\partial}{\partial\mathbf{n}}\frac{1}{|P-P_0|}d\sigma_2 + \iint_{S_{int}} q_1\frac{1}{|P-P_0|}dS_{int} + \\ &+\iint_{S_0}\phi_0\frac{\partial}{\partial\mathbf{n}}\frac{1}{|P-P_0|}dS_0 - \omega^2\iint_{S_0}\phi_0\frac{1}{|P-P_0|}dS_0 = 0; \quad P_0 \in S_{int}; \end{aligned}$$

$$\begin{aligned} &\iint_{\sigma_2}\phi_2\frac{\partial}{\partial\mathbf{n}}\frac{1}{|P-P_0|}d\sigma_2 + \iint_{S_{int}}\phi_{1i}\frac{\partial}{\partial\mathbf{n}}\frac{1}{|P-P_0|}dS_{int} + \iint_{S_{int}} q_1\frac{1}{|P-P_0|}dS_{int} + \\ &2\pi\phi_0(P_0) - \omega^2\iint_{S_0}\phi_0\frac{1}{|P-P_0|}dS_0 = 0; \quad P_0 \in S_0 \end{aligned}$$

Suppose, that there are n_1 points of collocation distributed on the surface σ_1; n_{12} – distributed on the interface surface S_{int}; n_2 points distributed on the surface σ_2 and n_0 points distributed on the free surface S_0. On each surface, beside S_{int}, the number of unknowns coincides with the number of collocation points. On the interface surface the number of unknowns equals twice the number of collocation points. So the total number of unknowns is $n_1 + 2n_{12} + n_2 + n_0$. This number coincides with number of equations in (13). It would be noted that $\frac{\partial}{\partial\mathbf{n}}\frac{1}{|P-P_0|} = 0$ if both points P and P_0 belong to S_{int}.

It would be noted that there are two types of kernels in the integral operators introduced above. Namely

$$\begin{aligned} A(S,\sigma)\psi &= \iint_S \psi\frac{\partial}{\partial\mathbf{n}}\frac{1}{|P-P_0|}dS; \\ B(S,\sigma)\psi &= \iint_S \psi\frac{1}{|P-P_0|}dS; \quad P_0 \in \sigma. \end{aligned} \tag{14}$$

Introducing denominations $\tilde{S}_1 = \sigma_1 = S_1 \cup S_{bot} \cup S_{baf}$, $\tilde{S}_2 = S_{int}$, $\tilde{S}_3 = \sigma_2 = S_2 \cup S_{baf}$ and $\tilde{S}_4 = S_0$ put them in the following expressions

$$A_{ij} = A(\tilde{S}_i, \tilde{S}_j); \quad B_{ij} = B(\tilde{S}_i, \tilde{S}_j).$$

So the system of integral equations (13) may rewritten in the following form

$$\begin{aligned} A_{11}\phi_1 + A_{12}\phi_{1i} &= B_{12}q_1; \quad P_0 \in \sigma_1; \\ A_{21}\phi_1 + A_{22}\phi_{1i} &= B_{22}q_1; \quad P_0 \in S_{int}; \end{aligned} \tag{15}$$

$$\begin{aligned} A_{32}\phi_{1i} + A_{33}\phi_2 + A_{34}\phi_0 - \omega^2 B_{34}\phi_0 &= -B_{32}q_1; \quad P_0 \in \sigma_2; \\ A_{22}\phi_{1i} + A_{23}\phi_2 + A_{24}\phi_0 - \omega^2 B_{24}\phi_0 &= -B_{22}q_1; \quad P_0 \in S_{int}; \\ A_{42}\phi_{1i} + A_{43}\phi_2 + A_{44}\phi_0 - \omega^2 B_{44}\phi_0 &= -B_{42}q_1; \quad P_0 \in S_0. \end{aligned}$$

From the first two equations in (15) one can obtain the expressions for φ_1 and φ_{1i} as following

$$\phi_1 = F_2 q_1; \quad \phi_{1i} = F_{2i} q_1. \tag{16}$$

Here

$$F_2 = A_\phi^{-1}B_{q_1}; \quad A_\phi = A_{11} - \frac{1}{2\pi}A_{12}A_{21}; \quad B_{q_1} = B_{12} - \frac{1}{2\pi}A_{12}B_{22};$$

$$F_{2i} = \frac{1}{2\pi}\left(B_{22} - A_{21}F_2\right).$$

Forth equation in (21) becomes

$$\phi_{1i} = \frac{1}{2\pi}\left(-A_{23}\phi_2 - A_{24}\phi_0 - B_{22}q_1 + \omega^2 B_{24}\phi_0\right); \quad P_0 \in S_{\text{int}}$$

Substituting this relation into third equation in (21) gives

$$\left(A_{33} - \frac{1}{2\pi}A_{32}A_{23}\right)\phi_2 = -\left(A_{34} - \frac{1}{2\pi}A_{32}A_{24}\right)\phi_0 - \left(B_{32} - \frac{1}{2\pi}A_{32}B_{22}\right)q_1 + \omega^2\left(B_{34} - \frac{1}{2\pi}A_{32}B_{24}\right)\phi_0; \quad P_0 \in \sigma_2.$$

So from third and forth two equations in (15) one can obtain the expressions for φ_2 and φ_{1i} as following

$$\begin{aligned}\phi_2 &= G_2 q_1 + \omega^2 G_3\phi_0 + G_4\phi_0\\ \phi_{1i} &= G_{2i} q_1 + \omega^2 G_{3i}\phi_0 + G_{4i}\phi_0\end{aligned} \tag{17}$$

Here

$$A_\phi = A_{33} - \frac{1}{2\pi}A_{32}A_{23}; \quad G_4 = -A_\phi^{-1}\left(A_{34} - \frac{1}{2\pi}A_{32}A_{24}\right);$$

$$G_2 = -A_\phi^{-1}\left(B_{32} - \frac{1}{2\pi}A_{32}B_{22}\right);$$

$$G_3 = A_\phi^{-1}\left(B_{34} - \frac{1}{2\pi}A_{32}B_{24}\right); \quad P_0 \in \sigma_2.$$

$$\begin{aligned}A_{32}\phi_{1i} + A_{33}\phi_2 + A_{34}\phi_0 - \omega^2 B_{34}\phi_0 &= -B_{32}q_1; \quad P_0 \in \sigma_2\\ A_{22}\phi_{1i} + A_{23}\phi_2 + A_{24}\phi_0 - \omega^2 B_{24}\phi_0 &= -B_{22}q_1; \quad P_0 \in S_{\text{int}};\\ A_{42}\phi_{1i} + A_{43}\phi_2 + A_{44}\phi_0 - \omega^2 B_{44}\phi_0 &= -B_{42}q_1; \quad P_0 \in S_0.\end{aligned}$$

$$\phi_{1i} = \frac{1}{2\pi}\left(-A_{23}\left(G_2 q_1 + \omega^2 G_3\phi_0 + G_4\phi_0\right) - A_{24}\phi_0 - B_{22}q_1 + \omega^2 B_{24}\phi_0\right);$$

$$G_{2i} = -\frac{1}{2\pi}\left(A_{23}G_2 + B_{22}\right); \quad G_{3i} = -\frac{1}{2\pi}\left(A_{23}G_3 - B_{24}\right);$$

$$G_{4i} = -\frac{1}{2\pi}\left(A_{23}G_4 + A_{24}\right).$$

Equating the two expressions for ϕ_{1l} from equations (16) and (17) it is possible to determine q_1 as follows

$$q_1 = \omega^2 D_3\phi_0 + D_4\phi_0; \tag{18}$$

$$\left(F_{2i} - G_{2i}\right)q_1 = \omega^2 G_{3i}\phi_0 + G_{4i}\phi_0;$$

$$D_3 = \left(F_{2i} - G_{2i}\right)^{-1} G_{3i}; \quad D_4 = \left(F_{2i} - G_{2i}\right)^{-1} G_{4i}$$

So

$$\begin{aligned}\phi_2 &= \Phi_\phi\phi_0 + \omega^2\Phi_\omega\phi_0;\\ \phi_{1i} &= \Phi_{\phi i}\phi_0 + \omega^2\Phi_{\omega i}\phi_0;\\ \Phi_\phi &= G_2 D_4 + G_4; \quad \Phi_\omega = G_2 D_3 + G_3;\\ \Phi_{\phi i} &= G_{2i} D_4 + G_{4i}; \quad \Phi_{\omega i} = G_{2i} D_3 + G_{3i}.\end{aligned}$$

Considering the fifth equation in (15) we have

$$\begin{aligned}&A_{42}\left(\Phi_{\phi i}\phi_0 + \omega^2\Phi_{\omega i}\phi_0\right) + A_{43}\left(\Phi_\phi\phi_0 + \omega^2\Phi_\omega\phi_0\right) + A_{44}\phi_0 - \omega^2 B_{44}\phi_0\\ &= -B_{42}\left(\omega^2 D_3 + D_4\right)\phi_0; \quad P_0 \in S_0.\end{aligned}$$

Finally obtain the following eigenvalue problem

$$A\phi_0 - \omega^2 B\phi_0 = 0,$$

where

$$\begin{aligned}A &= A_{42}\Phi_{\phi i} + A_{43}\Phi_\phi + A_{44} + B_{42}D_4;\\ B &= -A_{42}\Phi_{\omega i} - A_{43}\Phi_\omega + B_{44} - B_{42}D_3.\end{aligned}$$

It would be noted that proposed approach may be considered as variant of multi-domain BEM (MBEM) where the whole domain is divided into several subdomains for having better computational performance than using the single-domain BEM (SBEM).

5. Reducing to the System of One-Dimensional Equations

In formulas (14) the surfaces S and σ may be either different or coincident ones. If the surface S is the same as σ then integrals in (13) are singular and thus the numerical treatment of these integrals will have to take into account the presence of this integrable singularity. Integrands here are distributed strongly non-uniformly over the element and standard integration quadratures fail in accuracy. As in [14] replace the Cartesian co-ordinates (x, y, z) with cylindrical co-ordinates (r, θ, z), and integrate with respect to z and θ taking into account that

$$\left|P - P_0\right| = \sqrt{r^2 + r_0^2 + \left(z - z_0\right)^2 - 2rr_0\cos\left(\theta - \theta_0\right)}.$$

Use furthermore the cylindrical coordinate system and represent unknown functions as Fourier series by the circumferential coordinate

$$\psi\left(r, z, \theta\right) = \psi\left(r, z\right)\cos\alpha\theta; \quad i = 1, 2, \tag{19}$$

where α is a given integer (the number of nodal diameters).

In doing so we obtain the integral operators in following form

$$\iint_S \psi \frac{\partial}{\partial n}\frac{1}{|P-P_0|}dS = \int_\Gamma \psi(P)\Theta(P,P_0)d\Gamma;$$
$$\iint_S \psi \frac{1}{|P-P_0|}dS = \int_\Gamma \psi(P)\Phi(P,P_0)d\Gamma; \quad P_0 \in \sigma. \tag{20}$$

Here Γ is a generator of the surface S, kernels $\Theta(P,P_0)$ and $\Theta(P,P_0)$ are defined as following

$$\Theta(z,z_0) = \frac{4}{\sqrt{a+b}}\left\{\frac{1}{2r}\left[\frac{r^2-r_0^2+(z_0-z)^2}{a-b}\mathsf{E}_\alpha(k)-\mathsf{F}_\alpha(k)\right]n_r+\frac{z_0-z}{a-b}\mathsf{E}_\alpha(k)n_z\right\}$$

$$\Phi(P,P_0) = \frac{4}{\sqrt{a+b}}\mathsf{F}_\alpha(k).$$

The following notations are introduced hereinabove

$$\mathsf{E}_\alpha(k) = (-1)^\alpha(1-4\alpha^2)\int_0^{\pi/2}\cos 2\alpha\theta\sqrt{1-k^2\sin^2\theta}d\theta,$$
$$\mathsf{F}_\alpha(k) = (-1)^\alpha\int_0^{\pi/2}\frac{\cos 2\alpha\theta d\theta}{\sqrt{1-k^2\sin^2\theta}},$$
$$a = r^2+r_0^2+(z-z_0)^2, \quad b = 2rr_0;\ k^2 = \frac{2b}{a+b}.$$

Numerical evaluation of integral operators (20) was accomplished by the BEM with a constant approximation of unknown functions inside elements. It would be noted that internal integrals here are complete elliptic ones of first and second kinds. As the first kind elliptic integrals are non-singular, one can successfully use standard Gaussian quadratures for their numerical evaluation. For second kind elliptic integrals we have applied the approach based on the following characteristic property of the arithmetic geometric mean AGM(a, b) (see [18-20]):

$$\int_0^{\pi/2}\frac{d\theta}{\sqrt{a^2\cos^2\theta+b^2\sin^2\theta}} = \frac{\pi}{2AGM(a,b)}.$$

To define $AGM(a, b)$ there exist the simple Gaussian algorithm, described below,

$$a_0 = a; b_0 = b;\ a_1 = \frac{a_0+b_0}{2};$$
$$b_1 = \sqrt{a_0b_0};\ldots a_{n+1} = \frac{a_n+b_n}{2}; b_{n+1} = \sqrt{a_nb_n};\ldots$$
$$AGM(a,b) = \lim_{n\to\infty}a_n = \lim_{n\to\infty}b_n. \tag{21}$$

It is a very effective method to evaluate the elliptic integrals of the second kind. So we have the effective numerical procedures for evaluation of inner integrals, but external integrals in (20) have logarithmic singularities. So we treat these integrals numerically by special Gauss quadratures [17, 18] and apply the technique proposed in [21].

6. Some Numerical Results

6.1. Cylindrical Shells with Baffles

Consider the circular cylindrical shell with a flat bottom and having the following parameters: the radius is R = 1m, the thickness is h = 0.01m, the length L = 2m, Young's modulus $E = 2\cdot10^5$ MPa, Poisson's ratio ν = 0.3, the material's density is ρ = 7800 kg/m^3, the fluid density ρ_l = 1000 kg/m^3. The fluid filling level is denoted as H. The baffle is considered as a circle flat plate with a central hole (the ring baffle), a material's density is ρ = 7800 kg/m^3, the fluid density is ρ_l = 1000 kg/m^3. The fluid filling level is denoted as H.

The vertical coordinate of the baffle position (the baffle height) is denoted as H_1 ($H_1 < H$). The radius of the interface surface is denoted as R_2 (see Fig.1) and $H = H_1 + H_2$.

The numerical solution was obtained by using the BEM as it was described beforehand. In present numerical simulation we used 60 boundary elements along the bottom, 120 elements along wetted cylindrical parts and 100 elements along the radius of free surface. At the interface and baffle surfaces we used different numbers of elements depending on the radius of baffle.

Here we study the modes and frequencies of baffled tank in dependence of two parameters, R_2 and H_2. In numerical simulations consider different values both for R_2 and H_1.

First, perform the benchmark testing for the partially filled rigid cylindrical shell described above. The filling level was H=0.8 m.

Consider α=0. The analytical solution of R. Ibrahim [10] was used for comparison and validation. It can be expressed in the following form:

$$\frac{\chi_k^2}{g} = \frac{\mu_k}{R}\tanh\left(\mu_k\frac{H}{R}\right), \quad k = 1,2,\ldots;$$
$$\phi_k = J_0\left(\frac{\mu_k}{R}r\right)\cosh\left(\frac{\mu_k}{R}z\right)\cosh^{-1}\left(\frac{\mu_k}{R}H\right). \text{ b} \tag{22}$$

Here for α=0 values μ_k are roots of the equation $\frac{dJ_0(x)}{dx} = 0$, where $J_0(x)$ is Bessel function of the first kind, χ_k, ϕ_k are frequencies and modes of liquid sloshing in the rigid cylindrical shell.

Table 1 below provides the numerical values of the natural frequencies of liquid sloshing for nodal diameters α =0. The numerical results obtained with proposed MBEM were

compared with those received using formulae (22) and with results obtained using SBEM by K.G. Degtyarev et al [11].

Table 1. Comparison of analytical and numerical results.

		n=1	*n*=2	*n*=3	*n*=4	*n*=5
	SBEM	3.815	7.019	10.180	13.333	16.480
α=0	MBEM	3.816	7.017	10.177	13.330	16.480
	(22)	3.815	7.016	10.173	13.324	16.470

These results have been demonstrated the good agreement and testified the validity of proposed multi-domain approach.

Next, we have carried out the numerical simulation of the natural frequencies of liquid sloshing via the values of the interface surface radius R_2 at different position of the baffle H_1. At first calculate the natural frequencies of unbaffled tank at H=1.0m. These results were necessary for comparison with data of I. Gavrilyuk et al. [5].

Table 2 hereinafter provides the numerical values of the natural frequencies of liquid sloshing for nodal diameters α =0 and H=1.0m. The numerical results obtained with proposed MBEM were compared with those received using formulae (22).

Table 2. Comparison of analytical and numerical results at H=1.0m.

Modes	***n*=1**	***n*=2**	***n*=3**	***n*=4**	***n*=5**
MBEM	3.828	7.017	10.177	13.330	16.481
Analytical solution	3.828	7.016	10.173	13.324	16.471

To validate our multi-domain BEM approach we also have calculated the natural sloshing frequencies at H_1=H_2=0.5m and with R_2 =0.7m.

The comparison of results obtained with proposed MBEM and the analytically oriented approach presented by I. Gavrilyuk et al. in [11] has been demonstrated in Table 3.

Table 3. Comparison of numerical results for eigenvalues.

		n=1	*n*=2	*n*=3	*n*=4
H_1=0.5	MBEM	3.756	7.012	10.176	13.328
	[11]	3.759	7.010	10.173	13.324
H_1=0.9	MBEM	2.278	6.200	9.609	12.810
	[11]	2.286	6.197	9.608	12.808

These results also have demonstrated the good agreement and testified the validity of proposed multi-domain approach.

In all tables we have compared the eigenvalues $\omega^2 = \chi^2 / g$ of the problem described beforehand.

Figure 3 below demonstrates monotonic dependencies of the first 4 eigenvalues denoted over there as F1, F2, F3, F4 on the radius of the interface surface denoted by R2 at different baffle position H_1. From these results one can concluded that graphs of Fi as functions of R2 are essentially differ for different i and H_1. The presence of the baffle has affected drastically only on the lower frequencies. Also one can see that small baffles (when R_2 is relatively large) do not affect the lower frequencies. This conclusion corresponds to results of I. Gavrilyuk et al. [11].

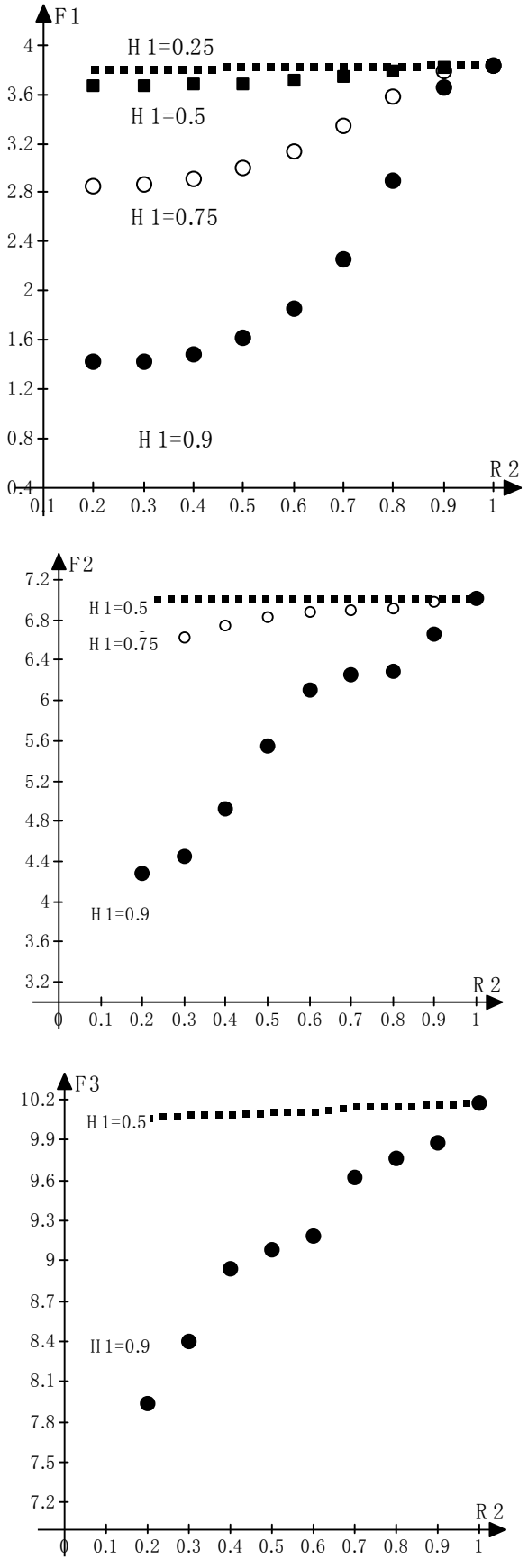

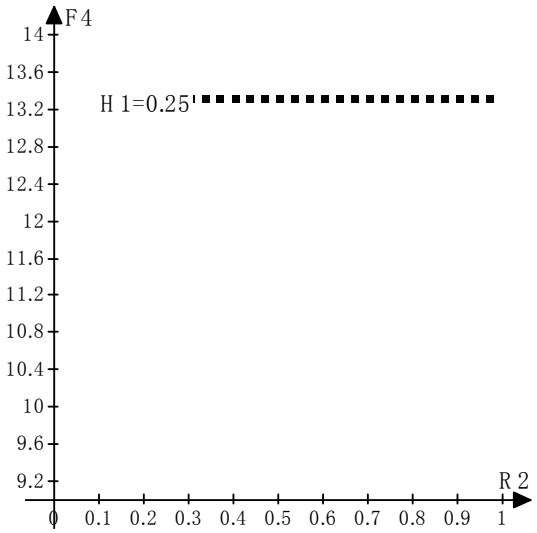

Figure 3. Eigenvalues versus R2 for H=1 and different H_1.

The three first modes of liquid vibrations are shown on Figure 4. Consider R2=0.2m.

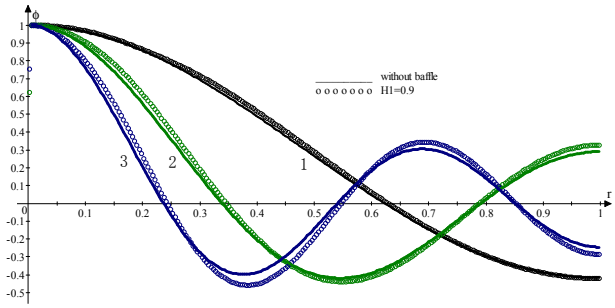

Figure 4. Modes of vibrations of un-baffled and baffled tanks.

Here numbers 1, 2, 3 correspond to the first, second and third modes. The value R2=0.2m was chosen based on data presented at Figure 3. Combination of R2=0.2m and H1=0.9 brings to frequencies' maximal decreasing. From these results one can conclude that modes of vibrations of baffled and un-baffled tanks are not differ significantly.

Consider α=1. In this case values μ_k are roots of the equation (see the handbook of I.S. Gradshteyn and I.M Ryzhik, [12])

$$\frac{dJ_1(x)}{dx} = 2\left[J_0(x) - J_2(x)\right],$$

Table 4 below provides the numerical values of the natural frequencies ($\omega^2 = \frac{\chi^2}{g}$) of liquid sloshing for nodal diameters α =1. The numerical results obtained with proposed MBEM were compared with those received using formulae (22) and with results obtained using SBEM by K.G. Degtyarev et al [11]. Consider H=0.8m.

Table 4. Comparison of analytical and numerical results.

		***n*=1**	***n*=2**	***n*=3**	***n*=4**	***n*=5**
	SBEM	1.657	5.332	8.538	11.709	14.868
α=1	MBEM	1.657	5.332	8.540	11.711	14.889
	(22)	1.657	5.329	8.536	11.706	14.864

Then we calculated the natural frequencies of un-baffled tank at H=1.0m and α=1. These results were necessary for comparison with data of I. Gavrilyuk et al. [5].

Table 5 hereinafter provides the numerical values of the natural frequencies of liquid sloshing for nodal diameters α =0 and H=1.0m. The numerical results obtained with proposed MBEM were compared with those received using formulae (22).

Table 5. Comparison of analytical and numerical results at H=1.0m and α=1.

Modes	***n*=1**	***n*=2**	***n*=3**	***n*=4**	***n*=5**
MBEM	1.750	5.332	8.538	11.709	14.870
(22)	1.750	5.331	8.536	11.706	14.864

Figure 5 below demonstrates monotonic dependencies of the first 4 eigenvalues for α=1 denoted over there as F1, F2, F3, F4 on the radius of the interface surface denoted by R2 at different baffle position H_1. From these results one can concluded that graphs of Fi (i=1, 2, 3, 4) as functions of R2 are essentially differ for different R_2 and H_1. The presence of baffle has affected drastically only on the lower frequencies. Also one can see that small baffles (when R_2 is relatively large) do not affect even the lower frequencies. This conclusion corresponds to results of I. Gavrilyuk et al. [11].

It would be noted that the values of frequencies both for α =0 and α =1 on the left vertical border of these graphs coincide with theoretical values for tanks with solid baffles at the same values of baffle position H_1. Here we have the boundary value problem for the two-compartment tank where the lower compartment is fully-filled with the liquid. But for this compartment the boundary value problem with zero Newman boundary condition was obtained. It leads to the ambiguous solution, but we have the known constant potential due to the known solution of the upper compartment with the mixed boundary value problem. For cylindrical shells this problem can be solved analytically. The liquid above the baffle behaves like a sloshing one while liquid below the baffle behaves like a rigid one.

On the right border of the graphs the values of frequencies coincide with ones obtained for the un-baffled tank.

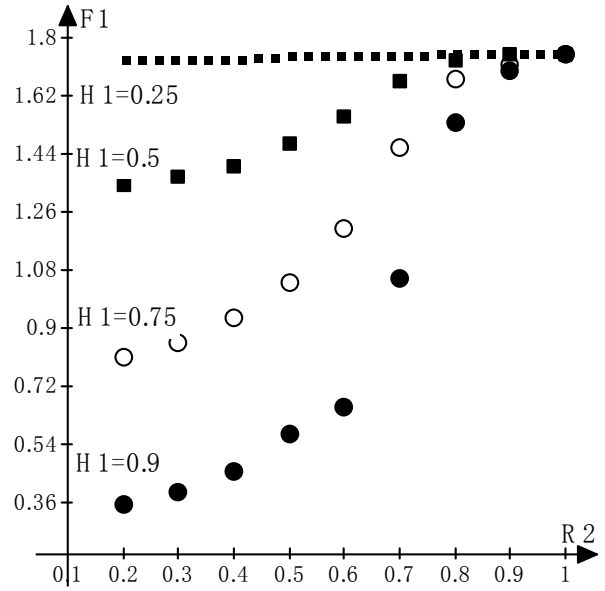

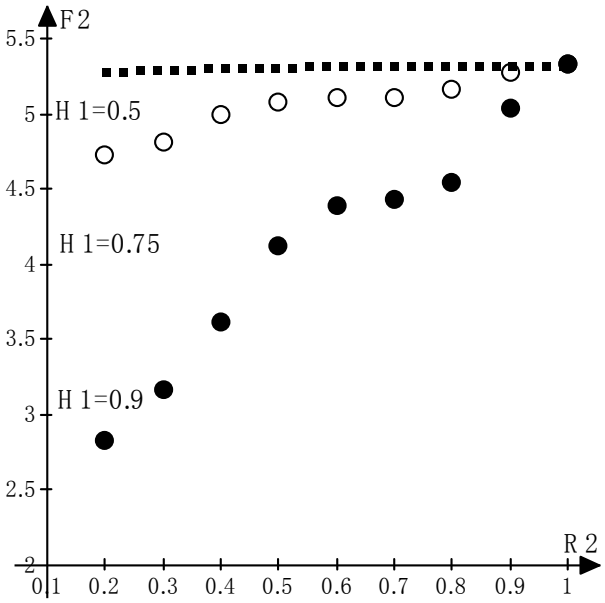

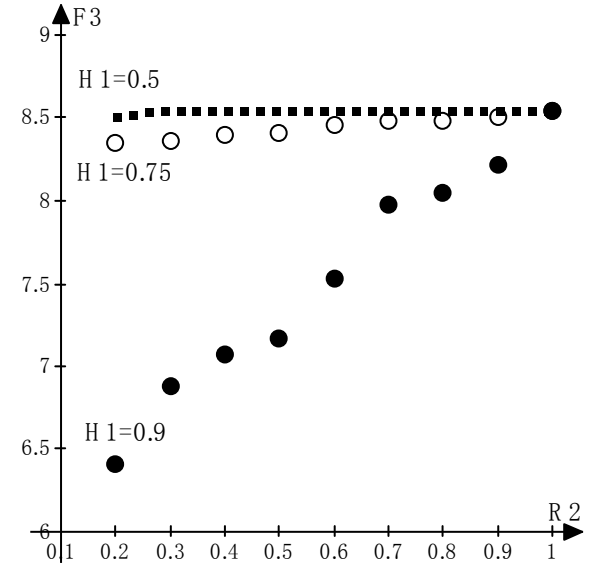

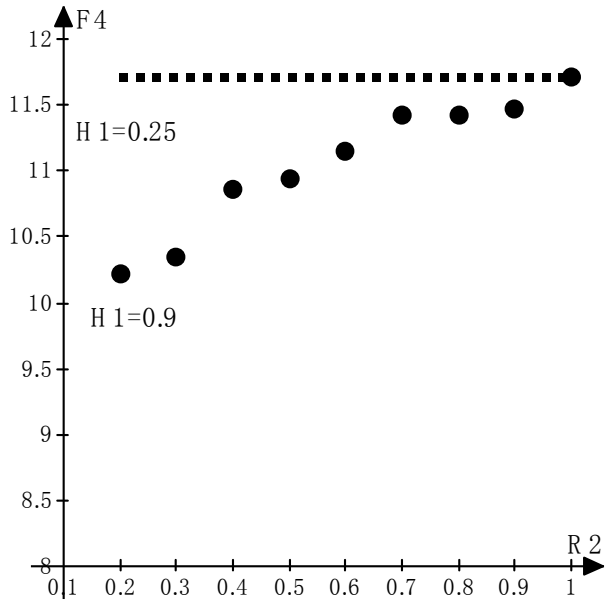

Figure 5. Eigenvalues at α=1 versus R2 for H=1 and different H_1.

The three first modes of liquid vibrations are shown on Figure 6. Here R2=0.2m and H_1=0.9m.

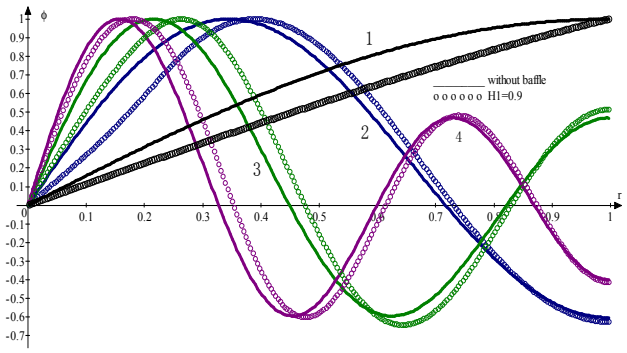

Figure 6. Modes of vibrations of un-baffled and baffled tanks, α=1.

Here numbers 1,2,3,4 correspond to the first, second, third and forth modes. These results demonstrate that modes of vibrations of baffled and un-baffled tanks at α=1 are differ more significantly than ones at α=0.

6.2. Conical Shells with Baffles

Conical shells in interaction with a fluid have received a little attention in scientific literature in spite of the usage of thin walled conical shells is of much importance in a number of different branches of engineering. In aerospace engineering such structures are used for aircraft and satellites. In ocean engineering, they are used for submarines, torpedoes, water-borne ballistic missiles and off-shore drilling rigs, while in civil engineering conical shells are used in containment vessels in elevated water tanks.

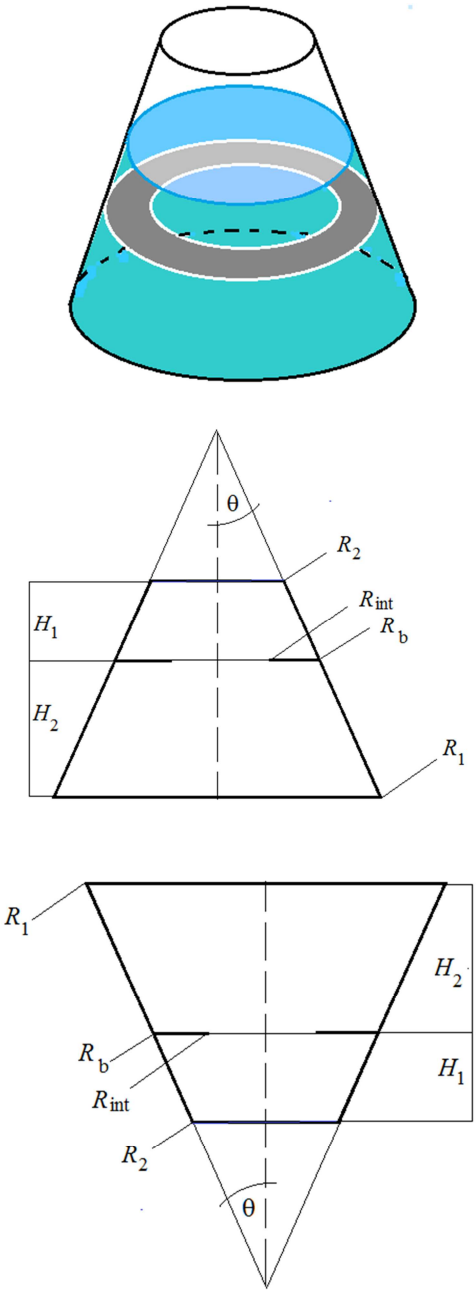

Figure 7. Baffled conical shells of Λ and V shapes.

The numerical procedure for a conical shell is the same as for a cylindrical one. The only distinction consists in formulas for the unit normal and coordinates of points at the considered solid surfaces. The first estimation was done for un-baffled coextensive cylindrical and conical shells with equal radiuses of free surfaces. For the cylindrical shell $R_1 = R_2 = 0.4$m and $H = 3.8464$m. That corresponds to the coextensive Λ-shape conical shell with $R_2 = 0.4$m and $R_1 = 1.0$m, $H=H_1+H_2=1.0392$m and $\theta=\pi/6$. These sizes were chosen for further comparison of our numerical results with data of I. Gavrilyuk et al. [13]. First, we have concluded that modes of liquid vibrations in both tanks are similar. These modes are shown on Figure 8.

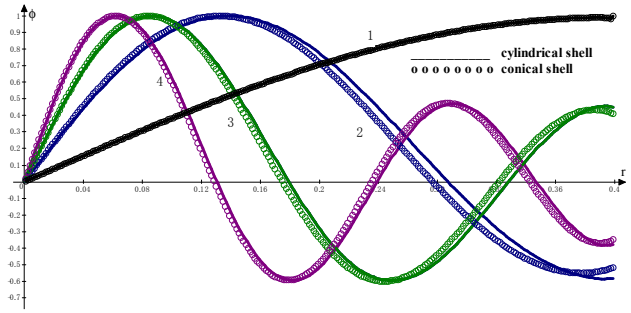

Figure 8. Modes of vibrations of the coextensive cylindrical and Λ-shape conical shells.

Here numbers 1, 2, 3 correspond to the first, second and third modes. Table 6 below provides the numerical values of the natural liquid sloshing frequencies at $\alpha = 1$ for the coextensive cylindrical and conical shells.

Table 6. Comparison of frequencies of the coextensive cylindrical and Λ-shape conical shells.

Modes	***n*=1**	***n*=2**	***n*=3**	***n*=4**	***n*=5**
Cylinder	4.6079	13.3504	21.3866	29.3409	37.3589
Cone	5.6206	13.9162	21.8827	29.7942	37.6864

As one can see from these results the only first frequency differs essentially for these tanks. Moreover, the first frequency of the cylindrical tank is less than this one of the Λ-shape conical tank. So it is possible to use namely this value at detuning the resonance frequency.

Next, the estimation was done for un-baffled coextensive cylindrical and V - shape conical tank with equal radiuses of free surfaces. For the cylindrical shell $R_1 = R_2 = 1$m and $H = 0.6154$ m. That corresponds to the coextensive V -shape conical shell with $R_2 = 1.$m and $R_1 = 0.4$m, $H=H_1+H_2=1.0392$m and $\theta=\pi/6$.

The modes of vibrations for both these tanks are shown on Figure 9, where numbers 1, 2, 3, 4 correspond to the first, second, third and forth modes. It would be noted that modes of the V – shape tank differ more essentially from those of the coextensive cylindrical tank as compared with the Λ-shape tank.

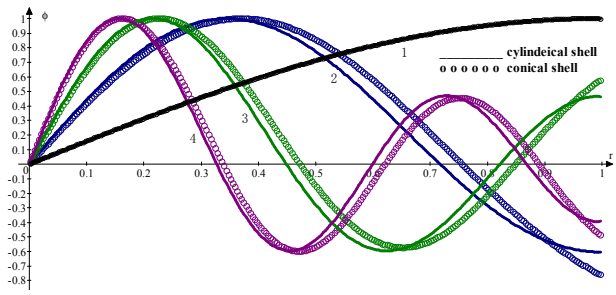

Figure 9. Modes of vibrations of the coextensive cylindrical and V -shape conical shells.

Table 7 provides the numerical values of the natural liquid

sloshing frequencies at α =1 for the coextensive cylindrical and V -shape conical shells.

Table 7. Comparison of frequencies of the coextensive cylindrical and V – shape conical shells.

Modes	*n*=1	*n*=2	*N*=3	*n*=4	*n*=5
Cylinder	1.4952	5.3163	8.5358	11.7059	14.8635
Cone	1.3052	4.9255	8.1411	11.3169	14.6724

The first frequencies differ essentially for both tanks and in this case the cylinder's first frequency is grater than that one of the V – shape conical tank. With increasing the frequency number *n* the difference between results became smaller.

As the next step *to validate our approach* we need to provide the comparing our numerical results with data obtained by I.Gavrilyuk et al. [13]. Our numerical simulation was dedicated to the frequencies $\omega_k^2 = \frac{\chi_k^2}{g}$ for α =0, 1,2 and k =1 because these are the lowest natural frequencies that give the essential contribution to the hydrodynamic load. In numerical simulation consider both V – shape and Λ-shape conical tanks and R_1 = 1.m and $\theta=\pi/6$. Noted, that for V – shape tank R_1 is the free surface radius, whereas for Λ-shape tank R_1 is the radius of bottom. If R_1, R_2 and θ are known quantities, than the corresponding value of H can be easy found as $H = (R_1 - R_2)\cot\theta$. In Table 8 the results of numerical simulation are presented for α =0, 1, 2 and different values of R_2. The comparison of results obtained by proposed method with data of I.Gavrilyuk et al. [13]. The results are in good agreement except the data for Λ – shape tank with for α =0 and R_2=0.2m. But was noted in [13] that in this case the low convergence was achieved using the proposed here analytical method.

Table 8. Natural frequencies of V – shape and Λ – shape conical tanks.

	V – shape					Λ – shape				
R_2	0.2	0.4	0.6	0.8	0.9	0.2	0.4	0.6	0.8	0.9
α =0, k =1										
[13]	3.386	3.386	3.382	3.139	2.187	24.153	10.014	6.665	4.550	2.683
MBEM	3.389	3.390	3.391	3.192	2.200	20.027	10.034	6.669	4.545	2.678
α =1, k =1										
[13]	1.304	1.302	1.254	0.934	0.542	11.332	5.629	3.515	1.661	0.726
MBEM	1.305	1.307	1.259	0.954	0.574	11.303	5.626	3.481	1.651	0.732
α =2, k =1										
[13]	2.263	2.263	2.255	2.015	1.361	17.760	8.967	5.941	3.724	1.923
MBEM	2.265	2.270	2.269	2.048	1.394	17.939	8.965	5.941	3.726	1.951

Next, we have carried out the numerical simulation of the natural frequencies of liquid sloshing for tanks with baffles. Both V – shape and Λ – shape baffled tanks were under consideration. Consider tanks of height H= H_1+H_2=1.0m at the different baffle position H_1. Here R_1 = 1.0m and R_2 = 0.5m for both type of tanks (see Figure 7).

In Table 9 the results of numerical simulation are presented for α =0, 1 and different baffle positions, described by the height H_1. Consider four eigenvalues for each α. The radius of the conical shell at the baffle position is denoted as R_b, and the free surface radius is R_{int} (see Figure 7). First, we have obtained the natural frequencies of V – shape and Λ – shape conical tanks without baffles. It corresponds to values H_1= H_2 =0.5m, R_{int}/R_b=1. The values of H_1 and H_2 can be arbitrary chosen but H_1+H_2=1.0m. Then we have put baffles at the different positions H_1=0.5m and H_1=0.8m and considered the different sizes of baffles, namely R_{int}/R_b=0.5 and R_{int}/R_b=0.2.

Table 9. Natural frequencies of V – shape and Λ – shape conical tanks with baffles.

n			1	2	3	4	1	2	3	4
H_1	H_2	R_{int}/R_b	V – shape				Λ – shape			
			α =0							
0.5	0.5	1	3.466	6.681	9.845	12.99	7.985	14.37	20.70	27.01
0.5	0.5	0.5	3.408	6.668	9.843	12.99	7.968	14.37	20.69	27.01
0.5	0.5	0.2	3.405	6.635	9.843	12.99	7.960	14.37	20.69	27.01
0.8	0.2	0.5	2.527	6.387	9.724	12.92	7.344	14.25	20.66	26.99
0.8	0.2	0.2	2.443	6.059	9.565	12.88	7.113	14.20	20.65	26.99
			α =1							
0.5	0.5	1	1.416	4.997	8.206	11.37	4.424	11.09	17.46	23.79
0.5	0.5	0.5	1.228	4.974	8.197	11.37	4.192	11.06	17.46	23.79
0.5	0.5	0.2	1.172	4.943	8.196	11.37	4.037	11.06	17.45	23.79
0.8	0.2	0.5	0.815	4.742	8.003	11.20	3.128	10.78	17.42	23.77
0.8	0.2	0.2	0.630	4.191	7.849	11.23	2.529	10.66	17.36	23.75

The modes of vibrations for V – shape tank for α =0 are shown on Figure 10, where numbers 1, 2, 3 correspond to the first, second and third forth modes. Solid lines correspond to the un-baffled tank and dotted lines correspond to the V – shape tank with baffle. Here H_1= 0.8m, H_2=0.2m, R_{int}/R_b=0.2, and R_1 = 1.0m, R_2 = 0.5.m.

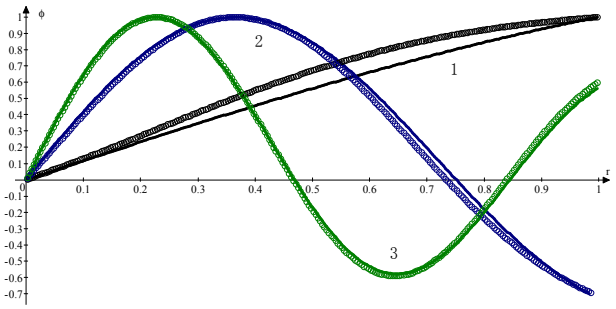

Figure 10. Modes of vibrations of the Λ and V -shape conical tanks with and without baffles.

From the results obtained show different behaviour of decreasing frequencies for V – shape and Λ – shape conical tanks. For Λ – shape tanks the baffle positions and their sizes are not affected essentially on the values of frequencies. For V – shape tanks the effects of baffle characteristics is more considerable.

It would be noted also that the first harmonic frequencies are lower than axisymmetric ones for both V – shape and Λ – shape conical tanks.

7. Conclusions

The proposed approach allows us to carry out the numerical simulation of baffled tanks with baffles of different sizes and with different position in the tank. This gives the possibility of governing the baffle radius and its position within the tank. The considered problem was solved using the multi-domain boundary element methods. The rigid baffles were considered. For baffles with holes the multi-domain approach was applied. Different behavior of frequencies for Λ and V-shape conical tanks with and without baffles was investigated. The first frequencies differ essentially for coextensive cylindrical and conical tanks. But modes of liquid vibrations in considered tanks are very close. The cylinder's first frequency is grater than that one of the V – shape conical tank. With increasing the frequency number *n* the difference between results became smaller.

It would be noted that dependencies of frequencies via the filling level at different values of gravity acceleration will be obtained numerically for vibrations of the fluid-filled tanks with and without baffles. This approach will be easy generalized for elastic tanks with elastic baffles. The geometry of tank also can be easy changed, so the results will be obtained for conical, spherical and compound shells.

References

[1] Robinson, H. G. R. and C. R. Hume. "Europa I: Flight Trial of F1- 5th June, 1964, 1964.

[2] Space Exploration Technologies Corp. "Demo Flight 2 Flight Review Update, June 15, 2007.

[3] G. Popov, S. Sankar, and T. S. Sankar, "Dynamics of liquid sloshing in baffled and compartmented road containers", J. Fluids Struct., no. 7, pp.803-821, 1993.

[4] Y. Guorong, and S. Rakheja S "Straight-line braking dynamic analysis of a partly-filled baffled and unbaffled tank truck", I. Mech. E., J. Auto Eng., vol. 223, pp. 11-26, 2009.

[5] N. Lloyd, E. Vaiciurgis, and T. A. G. Langrish, "The effect of baffle design on longitudinal liquid movement in road tankers: an experimental investig ation", Process Safety and Environ Prot Trans Inst. Chem. Engrs., vol. 80, no. 4, pp. 181-185, 2002.

[6] Guorong Yan, S. Rakheja, and K. Siddiqui, "Experimental study of liquid slosh dynamics in a partially filled tank," Trans. ASME, J. Fluids Eng., vol. 13, issue 1, 2009.

[7] L. Strandberg, Lateral stability of Road Tankers, National Road & Traffic Res. Inst. Report 138A, Sweden, 1978.

[8] M. F. Younes, Y. K. Younes, M. El-Madah, I. M. Ibrahim, and E. H. El-Dannanh, An experimental investigation of hydrodynamic damping due vertical baffle arrangements in rectangular tank, Proc. I Mech E, J. Eng. Maritime Environ., vol. 221, pp. 115-123, 2007.

[9] Bermudez, A., Rodrigues, R., Finite element analysis of sloshing and hydroelastic vibrations under gravity./ Mathematical Modelling and Numerical Analysis, Vol. 33, № 2, pp. 305-327, 1999.

[10] Gavrilyuk, I. Lukovsky I., Trotsenko, Yu. and Timokha, A. Sloshing in a vertical circular cylindrical tank with an annular baffle. Part 1. Linear fundamental solutions. Journal of Engineering Mathematics, vol. 54, pp. 71-88, 2006.

[11] Lloyd, N., Vaiciurgis, E. and. Langrish, T. A. G. The effect of baffle design on longitudinal liquid movement in road tankers: an experimental investigation. /Process Safety and Environ Prot Trans Inst. Chem. Engrs., vol. 80, no. 4, pp.181-185, 2002.

[12] Güzel, B. U., Gadinscak, M., Eren Semensigel, S., Turan, Ö. F., Control of Liquid Sloshing in Flexible Containers: Part 1. Added Masses; Part 2. Top Straps. /15th Australasia Fluid Mechanics Conference, Sydney, Australia, 8p., 2004.

[13] Gnitko V., Marchenko U., Naumenko V., Strelnikova E. Forced vibrations of tanks partially filled with the liquid under seismic load. Proc. of XXXIII Conference "Boundary elements and other mesh reduction methods" WITPress, Transaction on Modeling and Simulation, pp. 285-296, 2011. DOI: 10.2495/BE110251.

[14] Ventsel E.,. Naumenko V, Strelnikova E., Yeseleva E. Free vibrations of shells of revolution filled with a fluid. Engineering analysis with boundary elements, 34, pp. 856-862, 2010. DOI: 10.1016/j.enganabound.2010.05.004.

[15] K. Degtyarev, P. Glushich, V. Gnitko, E. Strelnikova. Numerical Simulation of Free Liquid-Induced Vibrations in Elastic Shells. // International Journal of Modern Physics and Applications. Vol. 1, No. 4, pp. 159-168, 2015. DOI: 10.13140/RG.2.1.1857.5209.

[16] Strelnikova E., Yeseleva E., Gnitko V., Naumenko V. Free and forced vibrations of the shells of revolution interacting with the liquid Proc. of XXXII Conference "Boundary elements and other mesh reduction methods" WITPress, Transaction on Modeling and Simulation, pp. 203-211, 2010.

[17] Brebbia, C. A., Telles, J. C. F. & Wrobel, L. C. Boundary Element Techniques, Springer-Verlag: Berlin and New York, 1984.

[18] K. G. Degtyarev, V. I. Gnitko, V.V. Naumenko, E. A. Strelnikova. BEM in free vibration analysis of elastic shells coupled with liquid sloshing. WIT Transaction on Modelling and Simulation, 2015, Vol. 61, pp. 35-46.

[19] David A. Cox. The Arithmetic-Geometric Mean of Gauss. *L'Enseignement Mathématique*, t. 30, pp. 275 -330, 1984.

[20] Stroud A. H., Secrest D. Gaussian Quadrature Formulas. Prentice-Hall, Englewood, N. J., Cliffs, 206 p., 1966.

[21] Naumenko V. V., Strelnikova H. A. Singular integral accuracy of calculations in two-dimensional problems using boundary element methods. Engineering analysis with boundary elements. №26, pp. 95-98, 2002 DOI: 10.1016/S0955-7997(01)00041-8.

[22] Ibrahim R. A. Liquid sloshing dynamics: theory and applications. Cambridge University Press, 957 p., 2005.

[23] Gavrilyuk, I. Lukovsky I., Trotsenko, Yu. and Timokha, A. Sloshing in a vertical circular cylindrical tank with an annular baffle. Part 1. Linear fundamental solutions. Journal of Engineering Mathematics vol.54, pp. 71-88, 2006.

[24] Gradshteyn, I. S.; Ryzhik, I. M.: Table of Integrals, Series and Products. Sixth Edition. Academic Press, 2000.

[25] Gavrilyuk, I., M. Hermann, Lukovsky I., Solodun O., Timokha, A. Natural Sloshing frequencies in Truncated Conical Tanks. Engineering Computations, Vol. 25 Iss: 6, pp. 518–540, 2008.